

On convergence of multiscale methods

Axel Målqvist Daniel Peterseim

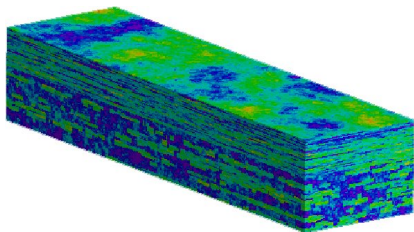
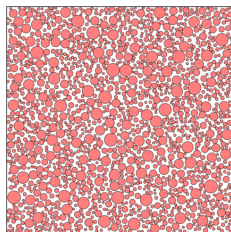
Uppsala University

Humboldt Universität

2012-09-20

Multiscale problems

Applications such as



- ▷ composite materials ▷ flow in a porous medium

require numerical solution of partial differential equations with rough data (module of elasticity, conductivity, or permeability).

Major challenge: Features on multiple non-separated scales.

Multiscale problems

Example: Oil reservoir simulation



Find pressure p and water concentration s such that:

$$-\nabla \cdot \mathbf{k} \mu(s) \nabla p = q, \quad \dot{s} - \nabla \cdot [f(s) \mu(s) \mathbf{k} \nabla p] = g,$$

where \mathbf{k} is permeability, $\mu(s)$ the total mobility, f fractional flow, and g, q sink and source terms.

Multiscale problems

Example: Oil reservoir simulation



Find pressure p and water concentration s such that:

$$-\nabla \cdot \mathbf{k} \mu(s_n) \nabla p_{n+1} = q, \quad \frac{s_{n+1} - s_n}{\Delta t} - \nabla \cdot [f(s_n) \mu(s_n) \mathbf{k} \nabla p_{n+1}] = g,$$

where \mathbf{k} is permeability, $\mu(s)$ the total mobility, f fractional flow, and g, q sink and source terms.

Multiscale problems

Example: Oil reservoir simulation



Find pressure p and water concentration s such that:

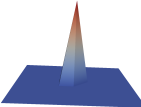
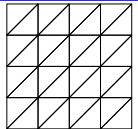
$$-\nabla \cdot k\mu(s_n)\nabla p_{n+1} = q, \quad \frac{s_{n+1} - s_n}{\Delta t} - \nabla \cdot [f(s_n)\mu(s_n)k\nabla p_{n+1}] = g,$$

where k is permeability, $\mu(s)$ the total mobility, f fractional flow, and g, q sink and source terms.

Finite elements (FE) – methodology

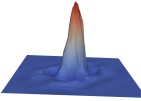
The numerical solution of PDEs by FEM consists of

- construction of an “appropriate” FE mesh
- choosing (local) basis functions (of variable degree of approximation)



An optimal construction should be adapted to the local behavior of the exact solution and, hence, should take into account

- local singularities of the solution
(e.g. singularities at re-entrant corners)
- effects of singular perturbations in the solutions
(e.g. boundary layers)
- scales and amplitudes of rough coefficients



Outline

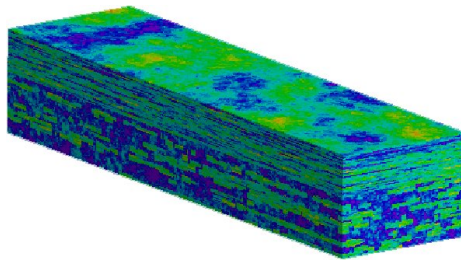
- ① Setting and Motivation
- ② Multiscale Method and Convergence
- ③ Full Discretization and Numerical Experiments
- ④ Adaptivity
- ⑤ Ongoing Work
- ⑥ Conclusion

Model multiscale problem

Poisson's equation

$$-\nabla \cdot A \nabla u = f \quad \text{in } \Omega \quad u = 0 \quad \text{on } \partial\Omega$$

with data $f \in L^2(\Omega)$ and $0 < \alpha \leq A \in L^\infty(\Omega)$

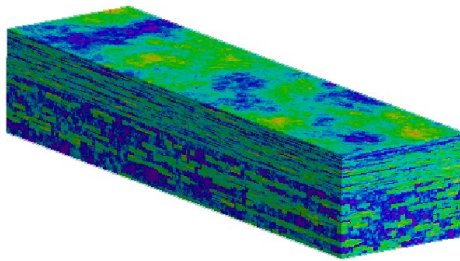


Model multiscale problem

Poisson's equation (variational form): $u \in V := H_0^1(\Omega)$ s.t.

$$a(u, v) := \int_{\Omega} (\textcolor{brown}{A} \nabla u) \cdot \nabla v \, dx = \int_{\Omega} f v \, dx =: F(v) \text{ for all } v \in V$$

with data $f \in L^2(\Omega)$ and $0 < \alpha \leq A \in L^\infty(\Omega)$



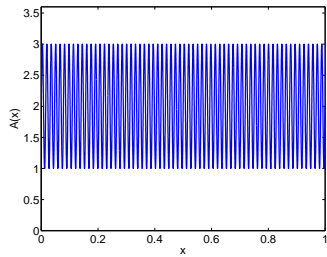
Model multiscale problem

Poisson's equation (variational form): $u \in V := H_0^1(\Omega)$ s.t.

$$a(u, v) := \int_{\Omega} (\mathbf{A} \nabla u) \cdot \nabla v \, dx = \int_{\Omega} f v \, dx =: F(v) \text{ for all } v \in V$$

with data $f \in L^2(\Omega)$ and $0 < \alpha \leq A \in L^\infty(\Omega)$

Example (periodic coefficient): $A(x) = 2 + \sin(2\pi x/\varepsilon)$, $\varepsilon = 2^{-6}$, $f = 1$



oscillatory coefficient

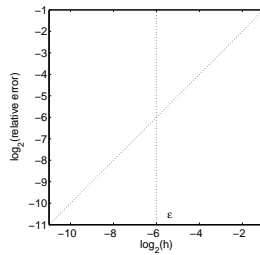
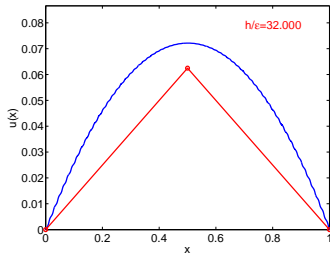
Model multiscale problem

Poisson's equation (variational form): $u \in V := H_0^1(\Omega)$ s.t.

$$a(u, v) := \int_{\Omega} (\mathbf{A} \nabla u) \cdot \nabla v \, dx = \int_{\Omega} f v \, dx =: F(v) \text{ for all } v \in V$$

with data $f \in L^2(\Omega)$ and $0 < \alpha \leq A \in L^\infty(\Omega)$

Example (periodic coefficient): $A(x) = 2 + \sin(2\pi x/\varepsilon)$, $\varepsilon = 2^{-6}$, $f = 1$



solution and P1-FEM-approximation

$\log_2(H^1(\Omega) - \text{error})$ vs. $\log_2(h)$



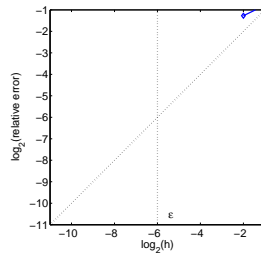
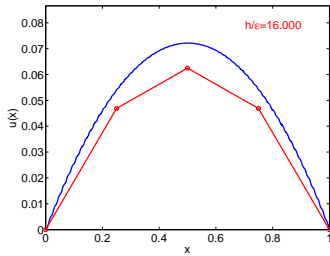
Model multiscale problem

Poisson's equation (variational form): $u \in V := H_0^1(\Omega)$ s.t.

$$a(u, v) := \int_{\Omega} (\mathbf{A} \nabla u) \cdot \nabla v \, dx = \int_{\Omega} f v \, dx =: F(v) \text{ for all } v \in V$$

with data $f \in L^2(\Omega)$ and $0 < \alpha \leq A \in L^\infty(\Omega)$

Example (periodic coefficient): $A(x) = 2 + \sin(2\pi x/\varepsilon)$, $\varepsilon = 2^{-6}$, $f = 1$



solution and P1-FEM-approximation

$\log_2(H^1(\Omega) - \text{error})$ vs. $\log_2(h)$

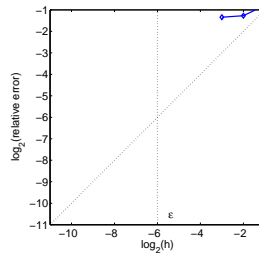
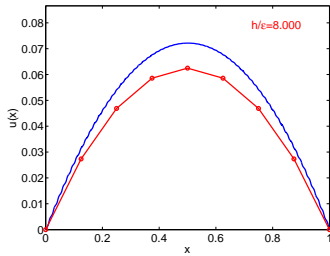
Model multiscale problem

Poisson's equation (variational form): $u \in V := H_0^1(\Omega)$ s.t.

$$a(u, v) := \int_{\Omega} (\mathbf{A} \nabla u) \cdot \nabla v \, dx = \int_{\Omega} f v \, dx =: F(v) \text{ for all } v \in V$$

with data $f \in L^2(\Omega)$ and $0 < \alpha \leq A \in L^\infty(\Omega)$

Example (periodic coefficient): $A(x) = 2 + \sin(2\pi x/\varepsilon)$, $\varepsilon = 2^{-6}$, $f = 1$



solution and P1-FEM-approximation

$\log_2(H^1(\Omega) - \text{error})$ vs. $\log_2(h)$



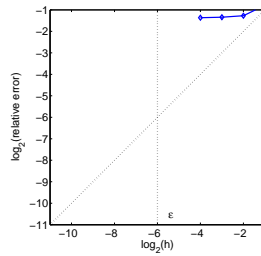
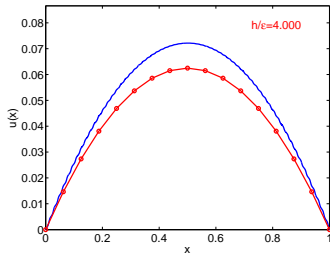
Model multiscale problem

Poisson's equation (variational form): $u \in V := H_0^1(\Omega)$ s.t.

$$a(u, v) := \int_{\Omega} (\mathbf{A} \nabla u) \cdot \nabla v \, dx = \int_{\Omega} f v \, dx =: F(v) \text{ for all } v \in V$$

with data $f \in L^2(\Omega)$ and $0 < \alpha \leq A \in L^\infty(\Omega)$

Example (periodic coefficient): $A(x) = 2 + \sin(2\pi x/\varepsilon)$, $\varepsilon = 2^{-6}$, $f = 1$



solution and P1-FEM-approximation

$\log_2(H^1(\Omega) - \text{error})$ vs. $\log_2(h)$



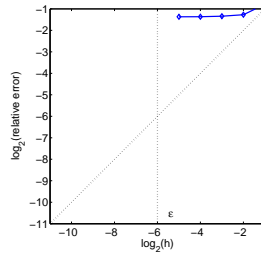
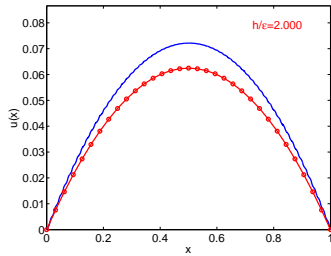
Model multiscale problem

Poisson's equation (variational form): $u \in V := H_0^1(\Omega)$ s.t.

$$a(u, v) := \int_{\Omega} (\mathbf{A} \nabla u) \cdot \nabla v \, dx = \int_{\Omega} f v \, dx =: F(v) \text{ for all } v \in V$$

with data $f \in L^2(\Omega)$ and $0 < \alpha \leq A \in L^\infty(\Omega)$

Example (periodic coefficient): $A(x) = 2 + \sin(2\pi x/\varepsilon)$, $\varepsilon = 2^{-6}$, $f = 1$



solution and P1-FEM-approximation

$\log_2(H^1(\Omega) - \text{error})$ vs. $\log_2(h)$



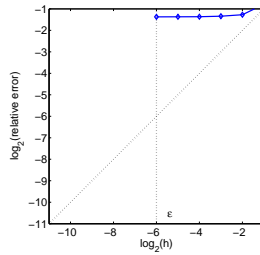
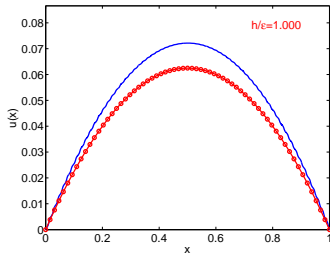
Model multiscale problem

Poisson's equation (variational form): $u \in V := H_0^1(\Omega)$ s.t.

$$a(u, v) := \int_{\Omega} (\mathbf{A} \nabla u) \cdot \nabla v \, dx = \int_{\Omega} f v \, dx =: F(v) \text{ for all } v \in V$$

with data $f \in L^2(\Omega)$ and $0 < \alpha \leq A \in L^\infty(\Omega)$

Example (periodic coefficient): $A(x) = 2 + \sin(2\pi x/\varepsilon)$, $\varepsilon = 2^{-6}$, $f = 1$



solution and P1-FEM-approximation

$\log_2(H^1(\Omega) - \text{error})$ vs. $\log_2(h)$



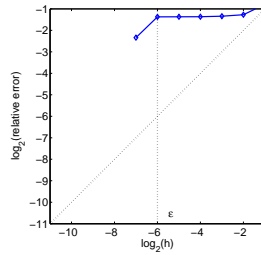
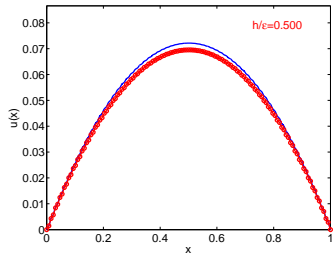
Model multiscale problem

Poisson's equation (variational form): $u \in V := H_0^1(\Omega)$ s.t.

$$a(u, v) := \int_{\Omega} (\mathbf{A} \nabla u) \cdot \nabla v \, dx = \int_{\Omega} f v \, dx =: F(v) \text{ for all } v \in V$$

with data $f \in L^2(\Omega)$ and $0 < \alpha \leq A \in L^\infty(\Omega)$

Example (periodic coefficient): $A(x) = 2 + \sin(2\pi x/\varepsilon)$, $\varepsilon = 2^{-6}$, $f = 1$



solution and P1-FEM-approximation

$\log_2(H^1(\Omega) - \text{error})$ vs. $\log_2(h)$



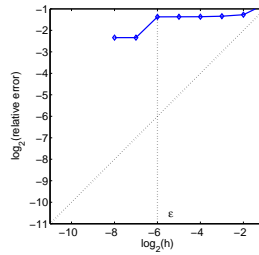
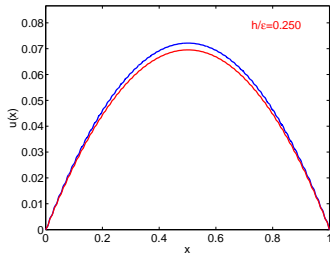
Model multiscale problem

Poisson's equation (variational form): $u \in V := H_0^1(\Omega)$ s.t.

$$a(u, v) := \int_{\Omega} (\mathbf{A} \nabla u) \cdot \nabla v \, dx = \int_{\Omega} f v \, dx =: F(v) \text{ for all } v \in V$$

with data $f \in L^2(\Omega)$ and $0 < \alpha \leq A \in L^\infty(\Omega)$

Example (periodic coefficient): $A(x) = 2 + \sin(2\pi x/\varepsilon)$, $\varepsilon = 2^{-6}$, $f = 1$



solution and P1-FEM-approximation

$\log_2(H^1(\Omega) - \text{error})$ vs. $\log_2(h)$



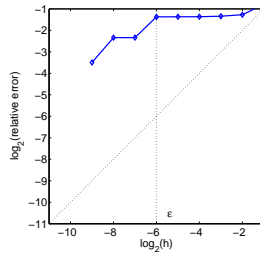
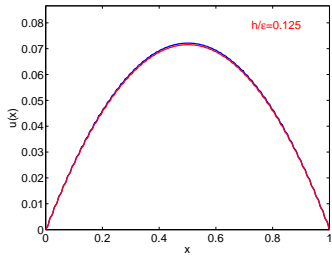
Model multiscale problem

Poisson's equation (variational form): $u \in V := H_0^1(\Omega)$ s.t.

$$a(u, v) := \int_{\Omega} (\mathbf{A} \nabla u) \cdot \nabla v \, dx = \int_{\Omega} f v \, dx =: F(v) \text{ for all } v \in V$$

with data $f \in L^2(\Omega)$ and $0 < \alpha \leq A \in L^\infty(\Omega)$

Example (periodic coefficient): $A(x) = 2 + \sin(2\pi x/\varepsilon)$, $\varepsilon = 2^{-6}$, $f = 1$



solution and P1-FEM-approximation

$\log_2(H^1(\Omega) - \text{error})$ vs. $\log_2(h)$



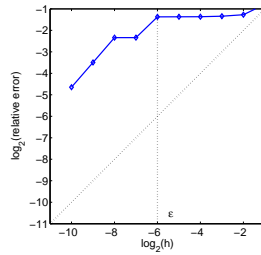
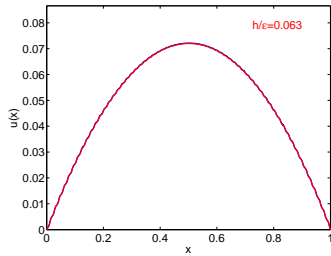
Model multiscale problem

Poisson's equation (variational form): $u \in V := H_0^1(\Omega)$ s.t.

$$a(u, v) := \int_{\Omega} (\mathbf{A} \nabla u) \cdot \nabla v \, dx = \int_{\Omega} f v \, dx =: F(v) \text{ for all } v \in V$$

with data $f \in L^2(\Omega)$ and $0 < \alpha \leq A \in L^\infty(\Omega)$

Example (periodic coefficient): $A(x) = 2 + \sin(2\pi x/\varepsilon)$, $\varepsilon = 2^{-6}$, $f = 1$



solution and P1-FEM-approximation

$\log_2(H^1(\Omega) - \text{error})$ vs. $\log_2(h)$



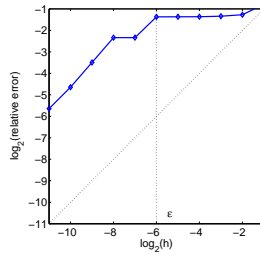
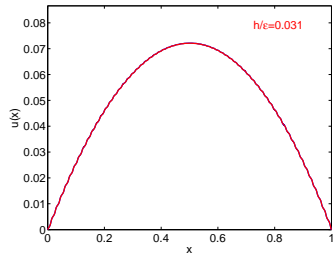
Model multiscale problem

Poisson's equation (variational form): $u \in V := H_0^1(\Omega)$ s.t.

$$a(u, v) := \int_{\Omega} (\mathbf{A} \nabla u) \cdot \nabla v \, dx = \int_{\Omega} f v \, dx =: F(v) \text{ for all } v \in V$$

with data $f \in L^2(\Omega)$ and $0 < \alpha \leq A \in L^\infty(\Omega)$

Example (periodic coefficient): $A(x) = 2 + \sin(2\pi x/\varepsilon)$, $\varepsilon = 2^{-6}$, $f = 1$



solution and P1-FEM-approximation

$\log_2(H^1(\Omega) - \text{error})$ vs. $\log_2(h)$



Model multiscale problem

Poisson's equation (variational form): $u \in V := H_0^1(\Omega)$ s.t.

$$a(u, v) := \int_{\Omega} (\textcolor{brown}{A} \nabla u) \cdot \nabla v \, dx = \int_{\Omega} f v \, dx =: F(v) \quad \text{for all } v \in V$$

with data $f \in L^2(\Omega)$ and $0 < \alpha \leq A \in L^\infty(\Omega)$

Examples (periodic coefficients)

- We have $\|u - u_h\| := \|A^{1/2} \nabla(u - u_h)\| \leq C(A, f)h = C'(f) \frac{h}{\epsilon}$.
- We need to resolve the fine scale features even to get the coarse scale behavior right.
- This implies that huge linear systems need to be solved in each time step in the oil reservoir application. Furthermore, the stiffness matrices changes in each time step.

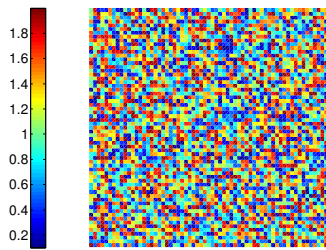
Model multiscale problem

Poisson's equation (variational form): $u \in V := H_0^1(\Omega)$ s.t.

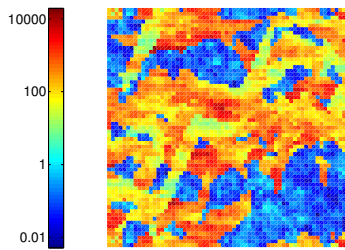
$$a(u, v) := \int_{\Omega} (\mathbf{A} \nabla u) \cdot \nabla v \, dx = \int_{\Omega} f v \, dx =: F(v) \text{ for all } v \in V$$

with data $f \in L^2(\Omega)$ and $0 < \alpha \leq A \in L^\infty(\Omega)$

Examples (rough coefficients)



random material (academic)



porous medium (SPE10 benchmark)

Objectives

Without any assumptions on scales ...

- Construction of an upscaled variational problem based on a generalized FEM
(coarse mesh \mathcal{T} of size H & modified nodal basis functions)
- Computation of basis functions involves solution of PDE only on local patches of coarse elements with diameter $\approx \log(1/H)$
- Error estimate

$$\|u - u_H^{\text{ms}}\| := \|A^{1/2} \nabla(u - u_H^{\text{ms}})\| \leq C(f)H$$

with $C(f)$ independent of scales of A



A. Målqvist and D. Peterseim.

Localization of Elliptic Multiscale Problems.

ArXiv e-prints, Oct. 2011.

Some known methods

- Upscaling techniques: Durlofsky et al. 98, Nielsen et al. 98
- Variational multiscale method: Hughes et al. 95, Arbogast 04, Larson-Målqvist 05, Nolen et al. 08, Nordbotten 09
- Multiscale FEM: Hou-Wu 96, Efendiev-Ginting 04, Aarnes-Lie 06
- Residual free bubbles: Brezzi et al. 98
- Multiscale finite volume method: Jenny et al. 03
- Heterogeneous multiscale method: Engquist-E 03, E-Ming-Zhang 04, Ohlberger 05
- Equation free: Kevrekidis et al. 05
- Metric based upscaling: Owhadi et al. 06
- ...

Common idea

Local approximations (in parallel) on a fine scale are used to modify a coarse scale space or equation

Some known methods

- Upscaling techniques: Durlofsky et al. 98, Nielsen et al. 98
- Variational multiscale method: Hughes et al. 95, Arbogast 04, Larson-Målqvist 05, Nolen et al. 08, Nordbotten 09
- Multiscale FEM: Hou-Wu 96, Efendiev-Ginting 04, Aarnes-Lie 06
- Residual free bubbles: Brezzi et al. 98
- Multiscale finite volume method: Jenny et al. 03
- Heterogeneous multiscale method: Engquist-E 03, E-Ming-Zhang 04, Ohlberger 05
- Equation free: Kevrekidis et al. 05
- Metric based upscaling: Owhadi et al. 06
- ...

Remark

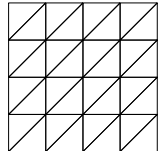
Error analysis rely on strong assumptions such as scale separation and periodicity

Outline

- 1 Setting and Motivation
- 2 **Multiscale Method and Convergence**
- 3 Full Discretization and Numerical Experiments
- 4 Adaptivity
- 5 Ongoing Work
- 6 Conclusion

Multiscale decomposition

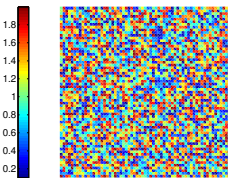
- (coarse) FE mesh \mathcal{T} with parameter H
- P1-FE space $V_H := \{v \in V \mid \forall T \in \mathcal{T}, v|_T \in P_1(T)\}$
- $\mathfrak{I}_{\mathcal{T}} : V \rightarrow V_H$ quasi-interpolation operator



Decomposition

$$V = V_H \oplus V^f \quad \text{with } V^f := \text{kernel } \mathfrak{I}_{\mathcal{T}} = \{v \in V \mid \mathfrak{I}_{\mathcal{T}} v = 0\}$$

Example:



rough coefficient

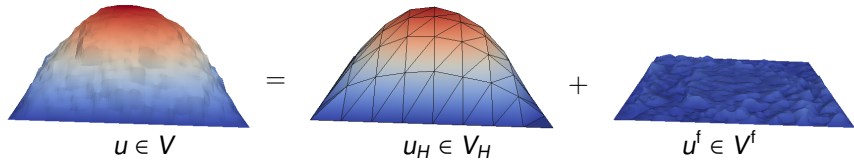
Multiscale decomposition

- (coarse) FE mesh \mathcal{T} with parameter H
- P1-FE space $V_H := \{v \in V \mid \forall T \in \mathcal{T}, v|_T \in P_1(T)\}$
- $\mathfrak{I}_{\mathcal{T}} : V \rightarrow V_H$ quasi-interpolation operator

Decomposition

$$V = V_H \oplus V^f \quad \text{with } V^f := \text{kernel } \mathfrak{I}_{\mathcal{T}} = \{v \in V \mid \mathfrak{I}_{\mathcal{T}} v = 0\}$$

Example:



Orthogonalization

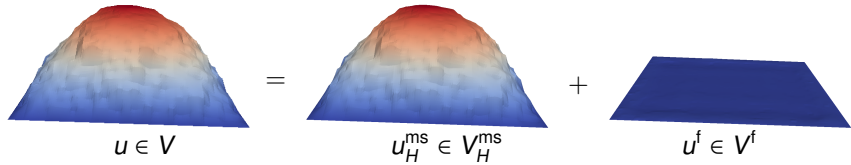
- For each $v \in V_H$ define finescale projection $\mathfrak{F}v \in V^f$ by

$$a(\mathfrak{F}v, w) = a(v, w) \quad \text{for all } w \in V^f$$

Orthogonal Decomposition

$$V = V_H^{\text{ms}} \oplus V^f \quad \text{with } V_H^{\text{ms}} := (V_H - \mathfrak{F}V_H)$$

Example:



Error analysis (perfect decomposition)

Lemma

$$|||u - u_H^{\text{ms}}||| \leq C_{\text{ol}} C_{\mathfrak{I}_{\mathcal{T}}} \alpha^{-1} \|Hf\|_{L^2(\Omega)}$$

Sketch of proof:

- recall $\|v - \mathfrak{I}_{\mathcal{T}}v\|_{L^2(T)} \leq C_{\mathfrak{I}_{\mathcal{T}}} H \|\nabla v\|_{L^2(\omega_T)}$ with
 $\omega_T := \cup\{K \in \mathcal{T} \mid T \cap K \neq \emptyset\}$ [Carstensen/Verfürth '99]
- orthogonal decomposition yields $u^f := u - u_H^{\text{ms}} \in V^f$
- $\mathfrak{I}_{\mathcal{T}}u^f = 0$, interpolation error estimate, and finite overlap of the patches ω_T conclude the proof

$$\begin{aligned} |||u^f|||^2 &= a(\underbrace{u^f + u_H^{\text{ms}}}_{=u}, u^f) = F(u^f) = F(u^f - \mathfrak{I}_{\mathcal{T}}u^f) \\ &\leq \sum_{T \in \mathcal{T}} \|f\|_{L^2(T)} \|u^f - \mathfrak{I}_{\mathcal{T}}u^f\|_{L^2(T)} \leq C_{\text{ol}} C_{\mathfrak{I}_{\mathcal{T}}} \alpha^{-1} \|Hf\|_{L^2(\Omega)} |||u^f||| \quad \square \end{aligned}$$

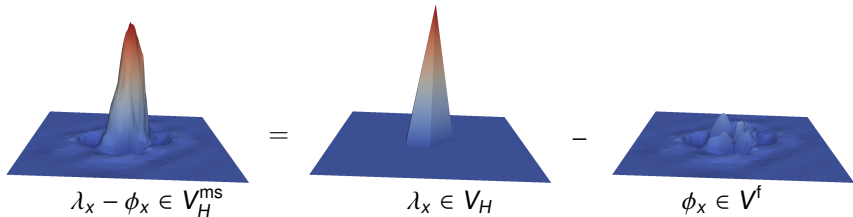
Modified nodal basis

- \mathcal{N} denotes set of interior vertices of \mathcal{T}
- $\lambda_x \in V_H$ denotes classical nodal basis function ($x \in \mathcal{N}$)
- $\phi_x = \mathfrak{F}\lambda_x \in V^f$ denotes finescale correction of λ_x ($x \in \mathcal{N}$)

Ideal multiscale FE space

$$V_H^{\text{ms}} = \text{span} \{ \lambda_x - \phi_x \mid x \in \mathcal{N} \}$$

Example



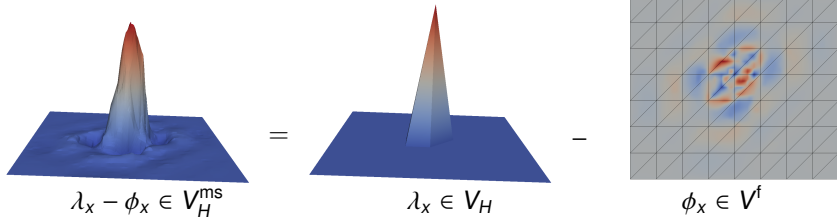
Modified nodal basis

- \mathcal{N} denotes set of interior vertices of \mathcal{T}
- $\lambda_x \in V_H$ denotes classical nodal basis function ($x \in \mathcal{N}$)
- $\phi_x = \mathfrak{F}\lambda_x \in V^f$ denotes finescale correction of λ_x ($x \in \mathcal{N}$)

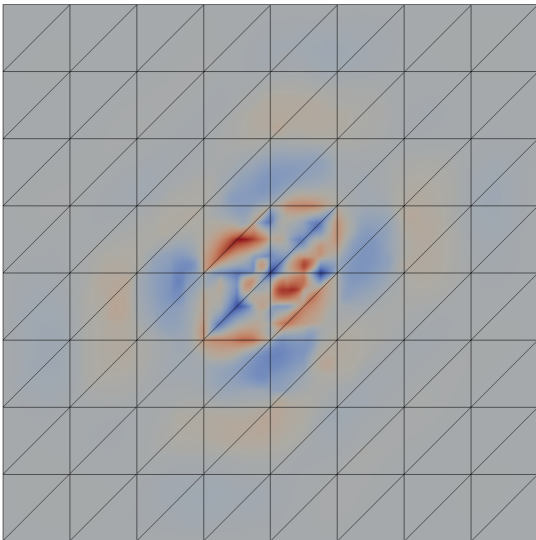
Ideal multiscale FE space

$$V_H^{\text{ms}} = \text{span} \{ \lambda_x - \phi_x \mid x \in \mathcal{N} \}$$

Example



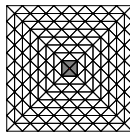
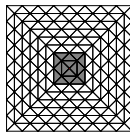
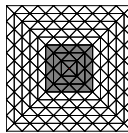
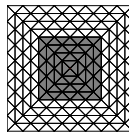
Modified nodal basis



Assuming more regularity on A we have $\lambda_x - \phi_x \in H^2(\Omega) \cap H_0^1(\Omega)$.

Localization

- Define nodal patches of k -th order $\omega_{x,k}$ about $x \in \mathcal{N}$

 $\omega_{x,1}$  $\omega_{x,2}$  $\omega_{x,3}$  $\omega_{x,4}$

- Localized corrections $\phi_{x,k} \in V^f(\omega_{x,k}) := \{v \in V^f \mid v|_{\Omega \setminus \omega_{x,k}} = 0\}$ solve

$$a(\phi_{x,k}, w) = a(\lambda_x, w) \quad \text{for all } w \in V^f(\omega_{x,k})$$

Localized multiscale FE spaces

$$V_{H,k}^{\text{ms}} = \text{span}\{\lambda_x - \phi_{x,k} \mid x \in \mathcal{N}\}$$

The multiscale method

Multiscale approximation seeks $u_{H,k}^{\text{ms}} \in V_{H,k}^{\text{ms}}$ such that

$$a(u_{H,k}^{\text{ms}}, v) = F(v) \quad \text{for all } v \in V_{H,k}^{\text{ms}}$$

Remarks:

- $\dim V_{H,k}^{\text{ms}} = |\mathcal{N}| = \dim V_H$
- basis functions of the multiscale method have local support and are totally independent
- overlap of the supports is proportional to the parameter k
- error analysis suggests $k \approx \log \frac{1}{H}$
- method can take advantage of periodicity

Error analysis

Lemma (Truncation error)

There exist $C_1 < \infty$ and $\gamma < 1$ independent of x, k, H such that

$$|||\phi_x - \phi_{x,k}||| \leq C_1 \gamma^k |||\phi_x|||.$$

Theorem (Main result)

$$|||u - u_{H,k}^{\text{ms}}||| \leq C_2 \left(k^d \|H^{-1}\|_{L^\infty(\Omega)} \gamma^k \|f\|_{L^2(\Omega)} + \|\mathcal{H}f\|_{L^2(\Omega)} \right)$$

holds with a constant C_2 that does not depend on H, k, f , or u .

Error analysis

Lemma (Truncation error)

There exist $C_1 < \infty$ and $\gamma < 1$ independent of x, k, H such that

$$|||\phi_x - \phi_{x,k}||| \leq C_1 \gamma^k |||\phi_x|||.$$

Theorem (Main result)

$$|||u - u_{H,k}^{\text{ms}}||| \leq C_2 \left(k^d \|H^{-1}\|_{L^\infty(\Omega)} \gamma^k \|f\|_{L^2(\Omega)} + \|\mathcal{H}f\|_{L^2(\Omega)} \right)$$

holds with a constant C_2 that does not depend on H, k, f , or u .

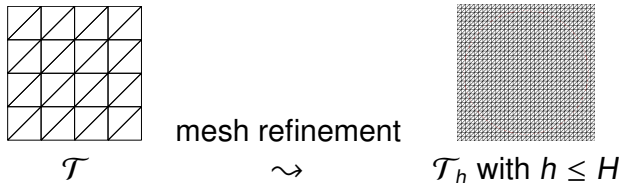
Theorem holds without any assumptions on scales or regularity!

Outline

- ① Setting and Motivation
- ② Multiscale Method and Convergence
- ③ **Full Discretization and Numerical Experiments**
- ④ Adaptivity
- ⑤ Ongoing Work
- ⑥ Conclusion

Full discretization

- Finescale mesh



- Reference FE space

$$V_h := \{v \in V \mid \forall T \in \mathcal{T}(\Omega), v|_T \in P_1(T)\}$$

- Reference FE solution $u_h \in V_h$ solves

$$a(u_h, v) = F(v) \quad \text{for all } v \in V_h$$

- Fully discrete corrections $\phi_{x,k}^h \in V_h^f(\omega_{x,k}) := V^f(\omega_{x,k}) \cap V_h$ satisfy

$$a(\phi_{x,k}^h, w) = a(\lambda_x, w) \quad \text{for all } w \in V_h^f(\omega_{x,k})$$

Full discretization

Fully discrete multiscale FE spaces

$$V_{H,k}^{\text{ms},h} = \text{span}\{\lambda_x - \phi_{x,k}^h \mid x \in \mathcal{N}\}$$

Fully discrete multiscale approximation $u_{H,k}^{\text{ms},h} \in V_{H,k}^{\text{ms},h}$ satisfies

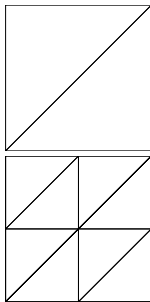
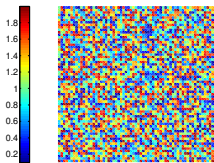
$$a(u_{H,k}^{\text{ms},h}, v) = F(v) \quad \text{for all } v \in V_{H,k}^{\text{ms},h}$$

Theorem (Error estimate)

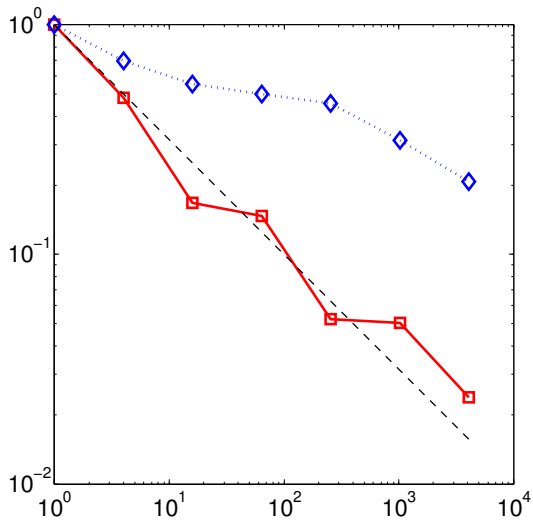
$$\|u - u_{H,k}^{\text{ms},h}\| \leq C_3 \left(\|u - u_h\| + k^d \|H^{-1}\|_{L^\infty(\Omega)} \gamma^k \|f\|_{L^2(\Omega)} + \|Hf\|_{L^2(\Omega)} \right)$$

holds with a constant C_3 that does not depend on H, h, k, f , or u .

Numerical experiment I

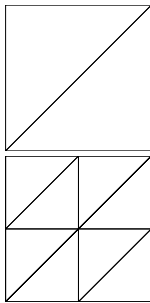
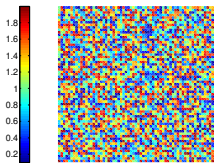


$$H = 2^{-1}, 2^{-2}, \dots, 2^{-7}$$
$$h = 2^{-9}, k = \log(1/H)$$

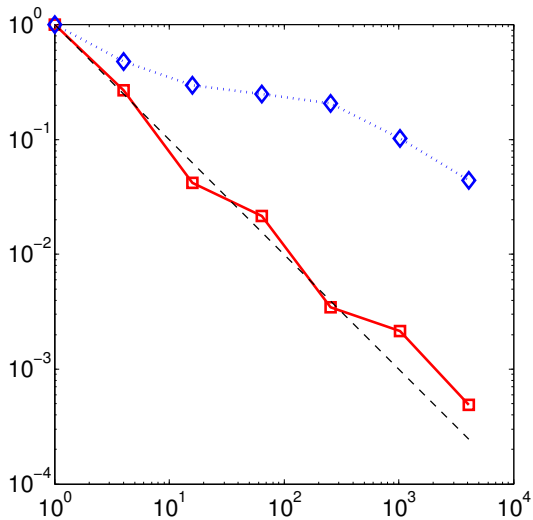


$\| \|u_h - u_{H,k}^{\text{ms},h}\| \|$ vs. #dof

Numerical experiment I

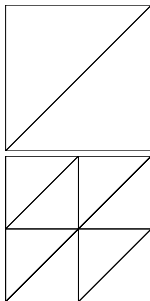
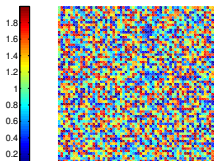


$$H = 2^{-1}, 2^{-2}, \dots, 2^{-7}$$
$$h = 2^{-9}, k = \log(1/H)$$

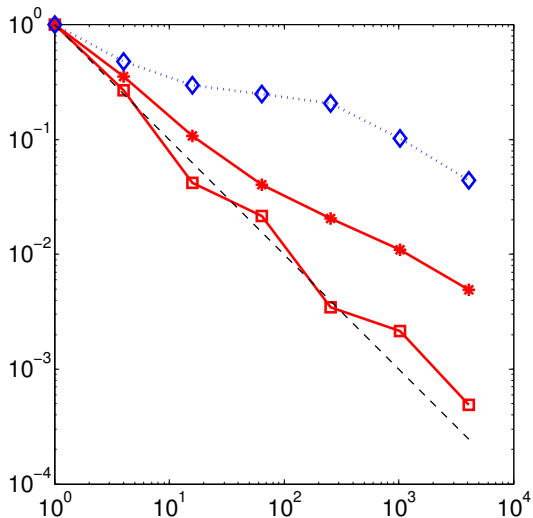


$\|u_h - u_{H,k}^{\text{ms},h}\|$ vs. #dof

Numerical experiment I

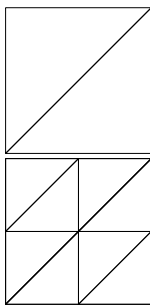
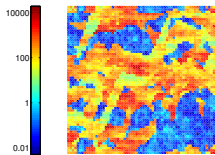


$$H = 2^{-1}, 2^{-2}, \dots, 2^{-7}$$
$$h = 2^{-9}, k = \log(1/H)$$

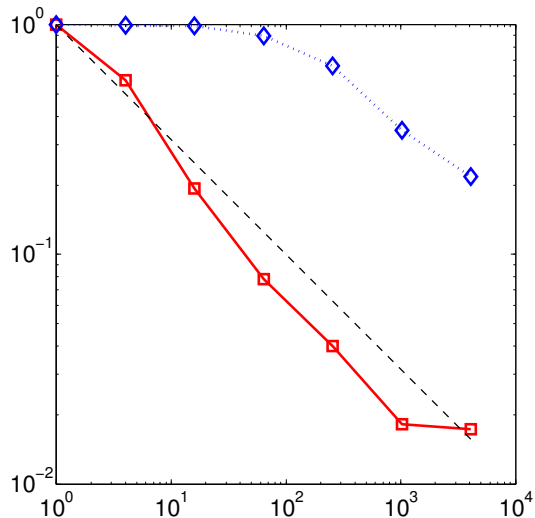


$\|u_h - \mathfrak{T}_\tau u_{H,k}^{\text{ms},h}\|$ vs. #dof

Numerical experiment II

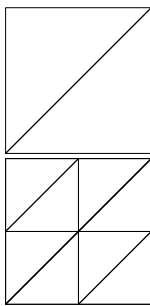
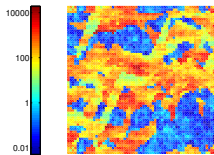


$$H = 2^{-1}, 2^{-2}, \dots, 2^{-7}$$
$$h = 2^{-9}, k = \log(1/H)$$



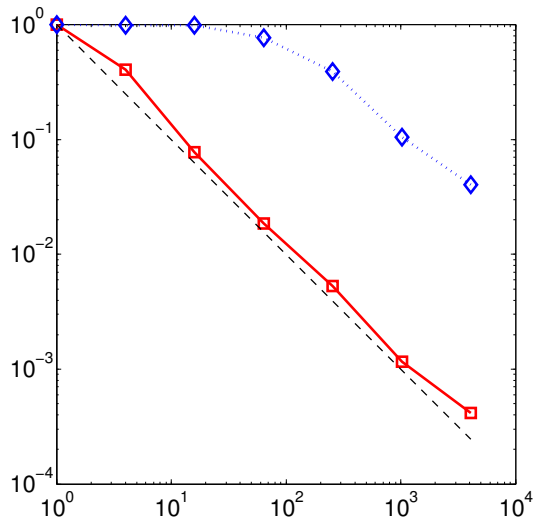
$\| \|u_h - u_{H,k}^{\text{ms},h}\| \|$ vs. #dof

Numerical experiment II



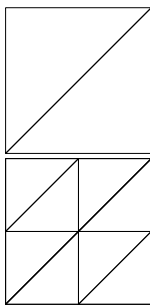
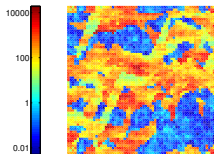
$$H = 2^{-1}, 2^{-2}, \dots, 2^{-7}$$

$$h = 2^{-9}, k = \log(1/H)$$



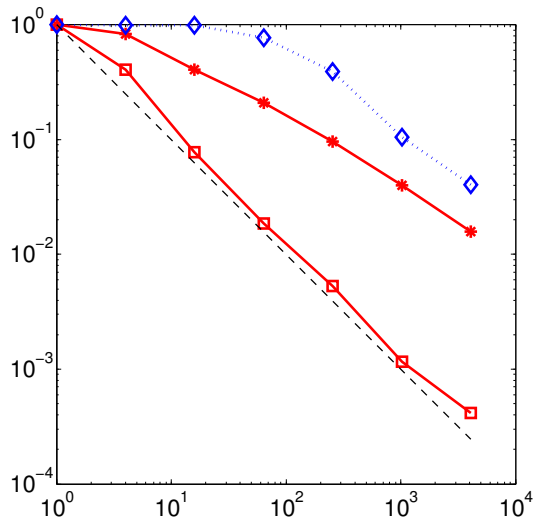
$\|u_h - u_{H,k}^{\text{ms},h}\|$ vs. #dof

Numerical experiment II



$$H = 2^{-1}, 2^{-2}, \dots, 2^{-7}$$

$$h = 2^{-9}, k = \log(1/H)$$



$\|u_h - \mathfrak{T}_\tau u_{H,k}^{\text{ms},h}\|$ vs. #dof

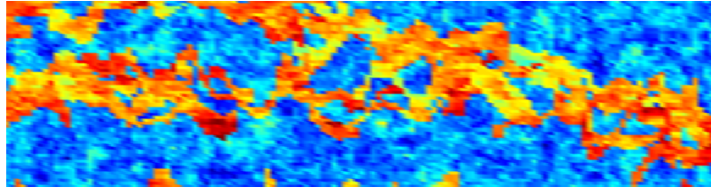
Outline

- 1 Setting and Motivation
- 2 Multiscale Method and Convergence
- 3 Full discretization and Numerical Experiments
- 4 **Adaptivity**
- 5 Ongoing Work
- 6 Conclusion

A posteriori error estimation and adaptivity

Motivation:

- The method we propose will have overlapping patches, which (especially in 3D) is expensive.
- The problems we consider often includes channels so the solution is typically somewhat localized in space.
- The size of the patches and the refinement level is difficult to predict a priori, we therefore need error indicators to tune these parameters automatically.



A posteriori error estimation and adaptivity

Let $\rho^2(v) = \sum_{K \in \mathcal{T}_h} h_K^2 \|\nabla \cdot A \nabla v\|_{L^2(K)}^2 + h_K \| [n \cdot A \nabla v] \|_{L^2(\partial K)}^2$.

Theorem

$$\begin{aligned} \|u - u_{H,k}^{\text{ms},h}\|^2 &\leq C \|Hf\|_{L^2(\Omega)}^2 + C(u_{H,k}^{\text{ms},h}) \sum_{x \in \mathcal{N}} \rho^2(\lambda_x - \phi_{x,k}^h) \\ &\quad + C(u_{H,k}^{\text{ms},h}) \sum_{x \in \mathcal{N}} H \|n \cdot A \nabla \phi_{x,k}^h\|_{L^2(\partial \omega_{x,k})}^2 \end{aligned}$$

- Effect of coarse mesh size included in first term.
- A standard element indicator on each patch measuring the effect of decreasing fine scale mesh size h .
- A new indicator on the boundary of each patch $\partial \omega_{x,k}$. The a priori analysis shows that $\phi_{x,k}^h$ decays exponentially in k .

A posteriori error estimation and adaptivity

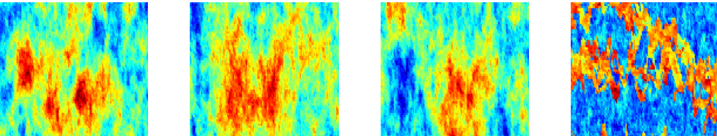
Let $\rho^2(v) = \sum_{K \in \mathcal{T}_h} h_K^2 \|\nabla \cdot A \nabla v\|_{L^2(K)}^2 + h_K \| [n \cdot A \nabla v] \|_{L^2(\partial K)}^2$.

Theorem

$$\begin{aligned} \|u - u_{H,k}^{\text{ms},h}\|^2 &\leq C \|Hf\|_{L^2(\Omega)}^2 + C(u_{H,k}^{\text{ms},h}) \sum_{x \in \mathcal{N}} \rho^2(\lambda_x - \phi_{x,k}^h) \\ &\quad + C(u_{H,k}^{\text{ms},h}) \sum_{x \in \mathcal{N}} H \|n \cdot A \nabla \phi_{x,k}^h\|_{L^2(\partial \omega_{x,k})}^2 \end{aligned}$$

- 1 Compute multiscale approximation, $u_{H,k}^{\text{ms},h}$.
- 2 Compute local error indicators.
- 3 If the error bound is small enough break.
- 4 Otherwise, decrease h locally if interior indicator is large and increase k locally if boundary indicator is large.
- 5 Go back to 1.

Numerical example

- Let the coarse mesh consist of 32×32 elements.
- Let the fine reference mesh consist of 256×256 elements.
- $f = -1$ in lower left corner ($0 \leq x, y \leq 1/128$) and $f = 1$ in upper right corner, otherwise $f = 0$.
- $A =$ 

We use a symmetric DG method as base for the multiscale method. Local problems are solved using Neumann boundary conditions, hanging nodes are allowed, there is a common reference mesh.

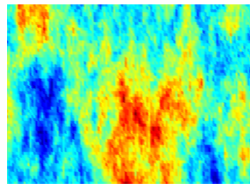


D. Elfversson, E. Georgoulis, and A. Målqvist.

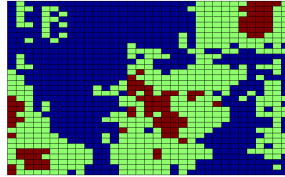
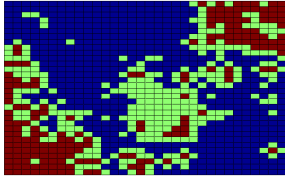
An adaptive discontinuous Galerkin multiscale method for elliptic problems,
Submitted to SIAM MMS.

Numerical example

We start with $h = H/2$ and $k = 2$ in all local problem. In each iteration we refine (divide h by 2) and increase (add 1 to k) 30% of the patches.

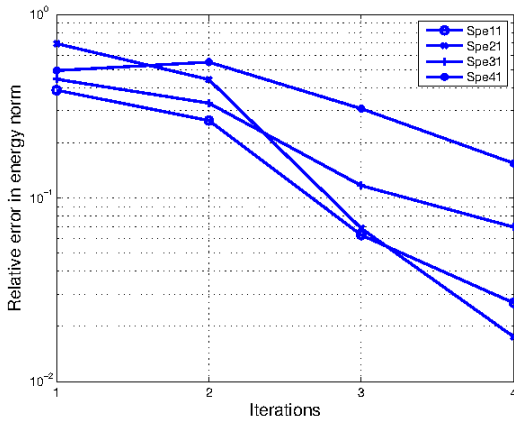


We plot h and k for SPE layer 31 after three iterations.



Numerical example

Convergence of relative error vs. number of iterations.



We note that SPE layer 41 is more difficult, $\max a / \min a \approx 6 \cdot 10^6$ instead of $6 \cdot 10^5$.

Why DG?

Advantage:

- It allows for Neumann conditions on the patches (leading to discontinuous basis functions).
- More flexibility in the adaptively refined local subgrids using hanging nodes.
- Construction of a conservative flux, which is essential in the application area, is easy.
- Can be applied on the coarse scale and combined with CG on the fine scale.

Disadvantage:

- Expensive.
- There is a penalty parameter which needs to be tuned.

Outline

- 1 Setting and Motivation
- 2 Multiscale Method and Convergence
- 3 Full discretization and Numerical Experiments
- 4 Adaptivity
- 5 **Ongoing Work**
- 6 Conclusion

Ongoing work

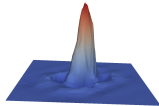
The key is to simplify the computation of the modified basis and to reuse the multiscale basis in the computation.

- Advection-diffusion-reaction equations.
- Semi-linear partial differential equations.
- Time dependent problems.

We will use the same construction as above for all these applications, namely: Find $\mathfrak{F}\lambda_x \in V^f$ such that

$$(A\nabla\mathfrak{F}\lambda_x, \nabla w) = (A\nabla\lambda_x, \nabla w), \quad \text{for all } w \in V^f,$$

$$V_H^{\text{ms}} = \text{span}(\{\lambda_x - \mathfrak{F}\lambda_x\}), \text{ and } x \in \mathcal{N}.$$



Advection-diffusion-reaction equations

Let $u \in V$ solve,

$$-\nabla \cdot A \nabla u + B \nabla u + Cu = f, \text{ in } \Omega \quad u = 0 \text{ on } \partial\Omega,$$

where $A, B, C \in L^\infty(\Omega)$ such that the problem is well posed.

It holds,

$$\begin{aligned} \|A^{1/2} \nabla(u - u_H^{\text{ms}})\|_{L^2(\Omega)}^2 &\lesssim \\ \alpha^{-1/2} \|H^{1+s} D^s f\|_{L^2(\Omega)} + \alpha^{-1} H &\left(\|B\|_{L^\infty(\Omega)} + H \|C - \nabla \cdot B\|_{L^\infty(\Omega)} \right) \|g\|_{H^{-1}(\Omega)}, \end{aligned}$$

with $s \leq 2$, for underlying finite elements of degree 1.

- Note that even for large advection and reaction terms we get good approximation, even though only A is considered in the construction of the basis.

Semi-linear PDE's

Let $u \in V$ solve,

$$-\nabla \cdot A \nabla u + F(u, \nabla u) = f, \text{ in } \Omega \quad u = 0 \text{ on } \partial\Omega,$$

where F is monotone and Lipschitz cont. in both arguments (L_F).

It holds,

$$\|A^{1/2} \nabla(u - u_H^{\text{ms}})\|_{L^2(\Omega)} \lesssim \alpha^{-1/2} \|H(f - \mathfrak{I}_T f)\|_{L^2(\Omega)} + \alpha^{-1} H L_F \|f\|_{H^{-1}(\Omega)}$$

without using information from F in the construction of the coarse multiscale space V_H^{ms} .

- For lowest order nonlinearity $F(u, \nabla u) = C(u)$ we even get $\alpha^{-1/2} \|H(f - \mathfrak{I}_T f)\|_{L^2(\Omega)} + \alpha^{-1} H^2 L_F \|f\|_{H^{-1}(\Omega)}$
- This means that the coarse basis can be used without modification throughout the full non-linear iteration.

Time dependent problems

Let $u \in V$ solve,

$$\dot{u} - \nabla \cdot A \nabla u = f, \text{ in } \Omega \quad u = 0 \text{ on } \partial\Omega,$$

with initial value $u(0) = 0$. For A independent of time we get,

$$\begin{aligned} \frac{1}{2} \|u(T) - u_H^{\text{ms}}(T)\|_{\Omega}^2 + \int_0^T \|A^{1/2} \nabla(u - u_H^{\text{ms}})\|_{L^2(\Omega)}^2 dt \\ \lesssim \alpha^{-2} \int_0^T \|H(f - \mathfrak{I}_T f)\|_{L^2(\Omega)}^2 dt. \end{aligned}$$

- The approximation is only discretized in space.
- With $A = A(t)$ one can discretize in time, and in each time step modify the basis if $A(t_{n+1}) - A(t_n)$ is large enough.

Oil reservoir simulation



Find pressure p and water concentration s such that:

$$-\nabla \cdot \mathbf{k} \mu(s) \nabla p = q, \quad \dot{s} - \nabla \cdot [f(s) \mu(s) \mathbf{k} \nabla p] = g.$$

A combination of these results will provide good insight into how to construct a multiscale method for the entire system.

Outline

- 1 Setting and Motivation
- 2 Multiscale Method and Convergence
- 3 Full discretization and Numerical Experiments
- 4 Adaptivity
- 5 Ongoing Work
- 6 Conclusion

Conclusion

- A new variational multiscale FEM yields scale-independent textbook convergence and, hence, establishes reliable computational approximation of multiscale problems.
- Numerical experiments confirms the theoretical results. Furthermore numerical results are not sensitive to high contrast.
- An adaptive algorithm for automatic tuning of critical method parameters is presented.
- Numerical examples confirms rapid decrease in error for very challenging permeability coefficients.
- Multiscale basis functions are very useful for many interesting applications such as, convection-diffusion-reaction problems, semi linear problems, and parabolic problems.

Outlook

- Treatment of high contrast also in the analysis, error bound for $\Im_{\mathcal{T}} u_{H,k}^{\text{ms},h}$, and error bounds in $L^2(\Omega)$ norm.
- Design and analysis of reliable multiscale methods hyperbolic problems.
- Design of a multiscale approach to the full two phase flow system.
- Consider **uncertainty** in the coefficient and construct efficient algorithms for computing statistical information, such as distribution function, of output quantities of interest.